

## Explosive destruction of $^{26}\text{Al}$

D. KAHL<sup>(1)</sup>(\*), H. YAMAGUCHI<sup>(2)</sup>, H. SHIMIZU<sup>(2)</sup>, K. ABE<sup>(2)</sup>, O. BELIUSKINA<sup>(2)</sup>,  
S. M. CHA<sup>(3)</sup>, K. Y. CHAE<sup>(3)</sup>, Z. GE<sup>(4)</sup>, S. HAYAKAWA<sup>(2)</sup>, M. S. KWAG<sup>(3)</sup>,  
D. H. KIM<sup>(5)</sup>, J. Y. MOON<sup>(6)</sup>, S. Y. PARK<sup>(5)</sup> and L. YANG<sup>(2)</sup>

<sup>(1)</sup> *School of Physics & Astronomy, the University of Edinburgh*

*James Clerk Maxwell Building, Peter Guthrie Tait Road, Edinburgh EH9 3FD, UK*

<sup>(2)</sup> *Center for Nuclear Study, the University of Tokyo, Wako Branch at RIKEN  
2-1 Hirosawa, Wako, Saitama 351-0198, Japan*

<sup>(3)</sup> *Department of Physics, Sungkyunkwan University - 300 Chunchun-dong,  
Jangan-gu, Suwon, Korea*

<sup>(4)</sup> *RIKEN Nishina Center, RIKEN - 2-1 Hirosawa, Saitama 351-0198, Japan*

<sup>(5)</sup> *Department of Physics, Ewha Womans University - Dae-Hyun-Dong,  
Seoul 120-750, Korea*

<sup>(6)</sup> *Wako Nuclear Science Center, KEK (The High Energy Accelerator Research Organization)  
2-1 Hirosawa, Wako, Saitama 351-0198, Japan*

received 28 November 2016

**Summary.** — The  $\gamma$ -ray emission associated with the radioactive decay of  $^{26}\text{Al}$  is one of the key pieces of observational evidence indicating stellar nucleosynthesis is an ongoing process in our Galaxy, and it was the first such radioactivity to be detected. Despite numerous efforts in stellar modeling, observation, nuclear theory, and nuclear experiment over the past four decades, the precise sites and origin of Galactic  $^{26}\text{Al}$  remain elusive. We explore the present experimental knowledge concerning the destruction of  $^{26}\text{Al}$  in massive stars. The precise stellar rates of neutron-induced reactions on  $^{26}\text{Al}$ , such as (n,p) and (n, $\alpha$ ), have among the largest impacts on the total  $^{26}\text{Al}$  yield. Meanwhile, reactions involving the short-lived isomeric state of  $^{26}\text{Al}$  such as radiative proton capture are highly-uncertain at present. Although we presented on-going experimental work from n\_TOF at CERN with an  $^{26}\text{Al}$  target, the present proceeding focuses only on the  $^{26}\text{Al}$  isomeric radioactive beam production aspect and the first experimental results at CRIB.

(\*) E-mail: [daid.kahl@ed.ac.uk](mailto:daid.kahl@ed.ac.uk)

## 1. – Introduction

$^{26}\text{Al}$  is among the most famous and well-studied nuclei in astrophysics. Along with observation of Tc in stellar spectra and neutrinos from SN 1987A and the Sun,  $^{26}\text{Al}$  is critical direct evidence demonstrating that nucleosynthesis continues in our Galaxy—and the stars that comprise it—to this day. Its ground state  $^{26\text{g}}\text{Al}$  has a half-life of  $7 \times 10^5$  yr, which is relatively short in terms of Galactic evolution, yet generally long enough for its ejection from a star to a transparent region where it can be observed.  $^{26\text{g}}\text{Al}$  has  $J^\pi = 5^+$ , and it predominately decays to the first excited state in  $^{26}\text{Mg}$ , which promptly de-excites by emitting a characteristic 1.809 MeV  $\gamma$ -ray. Combined, these two properties of  $^{26}\text{Al}$  are quite suitable for astronomical observation. However, from a nuclear physics perspective, the situation is complicated by a low-lying isomeric state  $^{26\text{m}}\text{Al}$  at 228 keV<sup>(1)</sup>; this  $J^\pi = 0^+$  isomer decays with a half-life of 6.3 seconds directly to the ground state of  $^{26}\text{Mg}$ . The extent to which these two states are connected by the nuclear trajectory and thermal transitions depends on both the nuclear properties (*e.g.* reaction rates) in this region of the chart of nuclides as well as the astrophysical environment (*e.g.* temperature). Although mechanisms to both produce and destroy (or bypass)  $^{26\text{g}}\text{Al}$  have been considered, historically the accepted observed mass of Galactic  $^{26}\text{Al}$  had been larger than the integrated calculations from a variety of stellar sources, putting a false bias on interest in the former. These days, purely by coincidence, estimates for the Galactic mass of  $^{26}\text{Al}$  fall towards the lower end of the previously adopted values, and considering all the sources purported to be possible contributors to the production of this radionuclide, the last decade has seen an increased interest in the destruction of  $^{26}\text{Al}$ .

Very little is known about the  $^{26\text{m}}\text{Al}(p,\gamma)$  stellar reaction rate, and in a sensitivity study on  $^{26}\text{Al}$  yields from massive stars, those authors were unable to do more than simply assume the proton radiative capture rate on the isomeric state was the same as for the ground state [1], despite the large spin-parity difference. Considering the short lifetime of  $^{26\text{m}}\text{Al}$ , reactions involving this species are only likely to be relevant during explosive stellar episodes. Our present knowledge concerning the properties of low-spin states above the isomeric proton threshold in  $^{27}\text{Si}$  is limited to a handful of studies. The first study was a  $\beta$ -delayed proton-decay of  $^{27}\text{P}$  which observed four resonances and assigned them tentatively as  $(1/2^+, 3/2^+)$  [2]. Two spectroscopic studies using the  $^{27}\text{Al}(^3\text{He},t)^{27}\text{Si}^*(p)^{26\text{m}}\text{Al}$  and  $^{28}\text{Si}(^3\text{He},\alpha)^{27}\text{Si}^*(p)^{26\text{m}}\text{Al}$  reactions observed over twenty levels with 3–5 keV resolution, as well as measuring  $\Gamma_p/\Gamma$  for several states to  $^{26\text{m}}\text{Al}$  [3]; however, the reported widths had a large systematic error of 34(19)% and are not absolute values. Finally, an in-beam  $\gamma$ -spectroscopy via the heavy-ion reaction  $^{12}\text{C}(^{16}\text{O},n)^{27}\text{Si}^*$  obtained excitation energies with typical resolution 0.5–1 keV, was able to determine or constrain  $J^\pi$  in most cases, and obtained lifetimes  $\tau$  for over fifty levels below or slightly above the proton threshold in  $^{27}\text{Si}$  [4]; in this case, the heavy-ion transfer reaction preferentially populates high-spin states owing to the incoming angular momentum, and no levels were observed which correspond to  $\ell = 0, 1$  proton capture on  $^{26\text{m}}\text{Al}$  within the supernova Gamow window of 3 GK ( $E_x > 8.2$  MeV). In summary, at present there is only limited information on  $J^\pi$  and no proton partial widths  $\Gamma_p$  are known for  $^{26\text{m}}\text{Al}$  resonances relevant for high-temperature explosive nucleosynthesis.

---

<sup>(1)</sup> In this paper we denote the nuclide in general  $^{26}\text{Al}$  and different states as  $^{26\text{g,m}}\text{Al}$  for the ground and isomeric states, respectively.

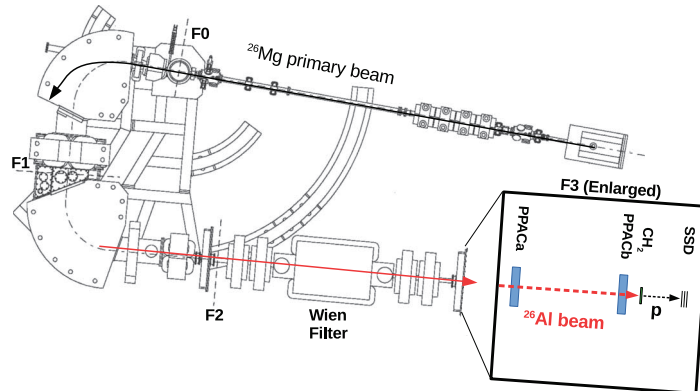


Fig. 1. – Schematic overhead view of the CRIB separator facility. The beam enters at the top right and experiments are conducted at F3. See main text.

## 2. – Experiment

Proton elastic scattering in inverse kinematics with an  $^{26\text{m}}\text{Al}$  radioactive ion beam (RIB) complements the existing studies. We will perform such a measurement in March 2017 at the Center for Nuclear Study low-energy RIB separator (CRIB) [5]. However, as such an RIB has never been produced at CRIB before the present work, we undertook a two-day machine test in July 2016 to check the production yield, purity, and phase-space parameters of  $^{26}\text{Al}$ . A schematic of the CRIB facility as well as the experimental setup is shown in fig. 1. A primary beam of  $^{26}\text{Mg}^{8+}$  was accelerated to 6.77 MeV/u by the RIKEN AVF cyclotron and arrived at the CRIB production target (F0) with a typical intensity of 20 p nA. The  $^{26}\text{Mg}$  beam impinged on the CRIB cryogenic production target [6], which was filled with 260 Torr of  $\text{H}_2$  gas at 90 K ( $0.7 \text{ mg}\cdot\text{cm}^{-2}$ ) and sealed with  $2.5 \mu\text{m}$  Havar foils, producing the RIB of interest via the  $^1\text{H}(^{26}\text{Mg}, ^{26}\text{Al})\text{n}$  reaction. These conditions were chosen to optimize production of  $^{26\text{m}}\text{Al}$  over  $^{26\text{g}}\text{Al}$  based on the literature cross-sectional data [7]. A sample particle identification plot at the achromatic focal plane F2 is shown in fig. 2.  $^{26}\text{Al}^{13+}$  production was optimized at  $119.6 \pm 1.5 \text{ MeV}$ . The Wien filter was set to  $\pm 60 \text{ kV}$  to purify the cocktail beam, and the main contamination was  $^{23}\text{Na}$  which can be easily distinguished from  $^{26}\text{Al}$ . The  $^{26}\text{Al}$  purity (as measured against different nuclides) was 80–90% at the experimental focal plane (F3). The typical intensity of  $^{26}\text{Al}$  was  $1 \times 10^5$  pps (at 25 p nA).

The setup at F3 consisted of two beam-line monitors (parallel plate avalanche counters, or PPACs), a  $7.5 \text{ mg}\cdot\text{cm}^{-2}$   $\text{CH}_2$  target, and a  $\Delta E$ - $E$  silicon telescope. The  $\Delta E$ - $E$  telescope was comprised of three layers, each with an active area of  $50 \times 50 \text{ mm}^2$ ; the first layer was  $73 \mu\text{m}$  with 16 orthogonal strips on each side (PSD1), while the second (SSD1) and third (SSD2) layers were both single-strip detectors of 1.5 mm thick each.

## 3. – Results

A key purpose of the machine test was to determine the *isomeric purity* of the cocktail beam. The isomeric purity is different from the  $^{26}\text{Al}$  purity; the former is  $^{26\text{m}}\text{Al}/^{26}\text{Al}$  whereas the latter is the total amount of all  $^{26}\text{Al}$  compared to *all nuclides* in the beam. CRIB does not have the capability to distinguish between  $^{26\text{g}}\text{Al}$  and  $^{26\text{m}}\text{Al}$  for individual

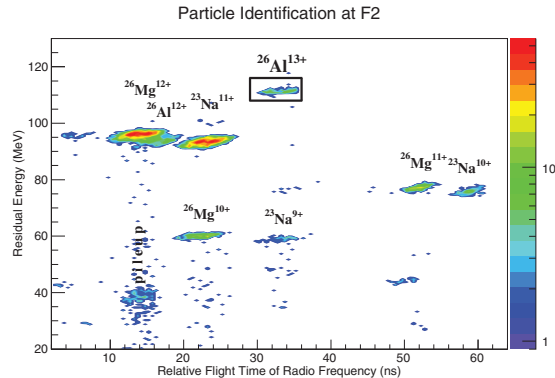


Fig. 2. – Particle identification of the cocktail beam at the achromatic focal plane F2. The abscissa shows relative flight time (F2 start, cyclotron RF stop) and the ordinate shows the residual ion energy as measured by a silicon detector. Only the fully-stripped  $^{26}\text{Al}^{13+}$  locus can be cleanly separated from the  $^{26}\text{Mg}$  primary beam. Note that the optical settings used to produce the above histogram are not optimized for  $^{26}\text{Al}$ , but rather illustrative of the largest array of species produced as well as the pattern of the particle identification.

ions, whereas we can uniquely identify each nuclear species event-by-event with our setup. The linchpin for our ability to perform a measurement of  $^{26\text{m}}\text{Al}$  proton elastic scattering is that high-purity  $^{26\text{g}}\text{Al}$  proton elastic scattering was previously measured and found to have no resonant structure within the experimental resolution [8]; this fact reduces our inability to uniquely identify the state of  $^{26}\text{Al}$  event-by-event to a matter of statistical background subtraction of the well-known Rutherford scattering cross section, provided we have a reliable determination of the isomeric purity.

To determine the isomeric purity, we performed a decay study by pulsing the primary beam in an on/off mode with a duty cycle of 12 s. When the beam was on, the cocktail beam was implanted into the  $\text{CH}_2$  target, and the trigger condition was PPACa downscaled by  $1 \times 10^3$ . When the beam was off, we measured  $\beta^+$  particles with the  $\Delta E$ - $E$  telescope, and the trigger was SSD1 OR SSD2. Considering the long half-life of  $^{26\text{g}}\text{Al}$  and that  $^{23}\text{Na}$  is stable, it is reasonable to assume that all  $\beta^+$  particles emitted from the target when the beam was off can be associated with the decay of  $^{26\text{m}}\text{Al}$ . Our preliminary measured half-life for the decay associated with these particles is 6.1 s as shown by the exponential fit in fig. 3(a); this value is consistent with the known  $^{26\text{m}}\text{Al}$  half-life of 6.3 seconds considering the time to turn the beam on and off is around 100 ms. The  $\beta^+$ -decay endpoint energy of  $^{26\text{m}}\text{Al}$  is 3.210 MeV. We did not find a  $\beta^+$  spectrum in the literature to compare our results with. Typically, the average  $\beta$  energy is around  $\frac{1}{3}$  of the endpoint, or 1.07 MeV in the case of  $^{26\text{m}}\text{Al}$  (the mean energy is generally shifted down for  $\beta^-$  decay and shifted up for  $\beta^+$  decay). The spectrum in fig. 3(b) shows a peak near 1.5 MeV and has nearly vanished by 3.2 MeV. Thus, our decay measurement is quite consistent with what is expected for  $\beta^+$  particles originating from the decay of  $^{26\text{m}}\text{Al}$  in both the time structure and energy spectrum obtained. Considering the number of decays we measured, the solid angle of the  $\Delta E$ - $E$  telescope, the implantation duty cycle, and the number of ions implanted, we find an isomeric purity of  $\geq 35\%$ . We anticipate that the developed  $^{26\text{m}}\text{Al}$  beam is satisfactory to observe low- $\ell$  proton resonances with large widths in the future.

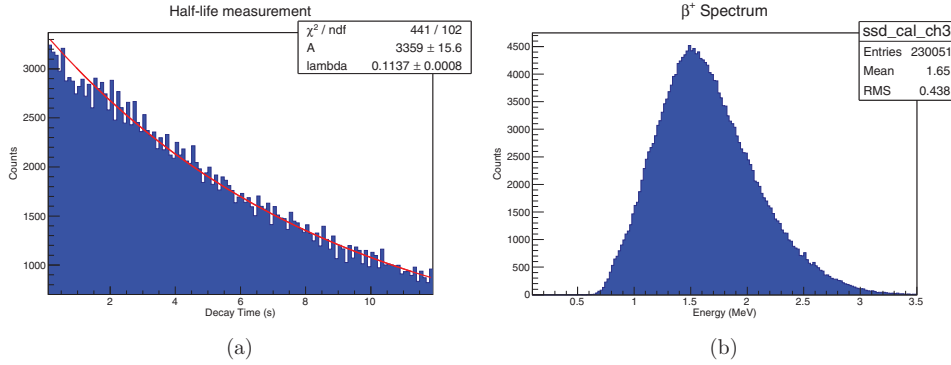


Fig. 3. – Preliminary results for the  $^{26\text{m}}\text{Al}$  decay measurement. (a) Decay time as measured for  $\beta^+$  particles at the SSDs and (b) the  $\beta^+$  energy spectrum. See main text.

\* \* \*

This work was partly supported by grants from the Science and Technology Facilities Council (STFC) in the United Kingdom, the JSPS KAKENHI (Grants No. 25800125 and 16K05369) in Japan, and grants from the National Research Foundation (NRF) funded by the Korea government (MEST) (No. NRF-2014S1A2A2028636, NRF-2015R1D1A1A01056918, NRF-2016K1A3A7A09005579, and NRF-2016R1A5A1013277). We also acknowledge the CNS and RIKEN staff for operation of the ion source and accelerator during the machine time.

## REFERENCES

- [1] ILIADIS C., CHAMPAGNE A., CHIEFFI A. and LIMONGI M., *Astrophys. J. Suppl.*, **193** (2011) 16.
- [2] OGNIBENE T. J., POWELL J., MOLTZ D. M., ROWE M. W. and CERNY J., *Phys. Rev. C*, **54** (1996) 1098.
- [3] DEIBEL C. M., CLARK J. A., LEWIS R., PARIKH A., PARKER P. D. and WREDE C., *Phys. Rev. C*, **80** (2009) 035806.
- [4] LOTAY G., WOODS P. J., SEWERYNIAK D., CARPENTER M. P., JANSSENS R. V. F. and ZHU S., *Phys. Rev. C*, **84** (2011) 035802.
- [5] YANAGISAWA Y., KUBONO S., TERANISHI T., UE K., MICHIMASA S., NOTANI M., HE J. J., OHSHIRO Y., SHIMOURA S., WATANABE S., YAMAZAKI N., IWASAKI H., KATO S., KISHIDA T., MORIKAWA T. and MIZOI Y., *Nucl. Instrum. Methods Phys. Res. A*, **539** (2005) 74.
- [6] YAMAGUCHI H., WAKABAYASHI Y., AMADIO G., HAYAKAWA S., FUJIKAWA H., KUBONO S., HE J. J., KIM A. and BINH D. N., *Nucl. Instrum. Methods Phys. Res. A*, **589** (2008) 150.
- [7] SKELTON R. T., KAVANAGH R. W. and SARGOOD D. G., *Phys. Rev. C*, **35** (1987) 45.
- [8] PITTMAN S. T., BARDAYAN D. W., CHAE K. Y., CHIPPS K. A., JONES K. L., KOZUB R. L., MATEI C., MATOS M., MOAZEN B. H., NESARAJA C. D., OMALLEY P. D., PAIN S. D., PARKER P. D., PETERS W. A., SHRINER J. F. jr. and SMITH M. S., *Phys. Rev. C*, **85** (2012) 065804.